Geological Society of America
Special Paper 306
1996

Meteoric water/rock ratios and the significance of sequence and parasequence boundaries in the Gobbler Formation (Middle Pennsylvanian) of south-central New Mexico

Thomas J. Algeo
H. N. Fisk Laboratory of Sedimentology, Department of Geology, University of Cincinnati, Cincinnati, Ohio 45221-0013

ABSTRACT

The upper carbonate member of the Middle Pennsylvanian Gobbler Formation of south-central New Mexico is composed of a succession of 3–20-m-thick (10–66 ft) parasequences exhibiting petrographic and isotopic evidence of subaerial exposure and early meteoric diagenesis at parasequence caps. Groups of four to six parasequences are arranged in 30–70-m-thick (100–230 ft) sequences that grade upward from marly basal members into grainy capping members exhibiting brecciation, karst solution features, and laminar and oxidized crusts. About 2‰–3‰ enrichment of micrite $\delta^{13}C$ values downward from individual parasequence tops reflects a decrease in average meteoric water/rock ratios from about 800 at parasequence caps to about 200 at a depth of 10 m, reflecting reduced fluid flux and/or evolution of fluid isotopic compositions downsection toward primary marine-carbonate values (+4.0‰ ± 0.5‰ $\delta^{13}C$). Depletion of micrite $\delta^{13}C$ values is somewhat stronger with respect to sequence boundaries than to parasequence boundaries in the Mockingbird Gap Hills section, indicating that the former represent surfaces of longer or more intense meteoric diagenesis than the latter.

INTRODUCTION

Despite extensive research on the internal architecture of sequences and parasequences (e.g., Vail, 1987; Posamentier et al., 1988; Sarg, 1988; Van Wagoner et al., 1988, 1990), the relation of diagenesis to sequence stratigraphic boundaries has received comparatively little attention (e.g., Driese et al., 1992). The Middle Pennsylvanian Gobbler Formation of south-central New Mexico offers an excellent case study for such diagenetic relations owing to an abundance of sequence boundaries (SBs) and parasequence boundaries (PSBs) that are readily identifiable and that exhibit evidence of strong early meteoric diagenesis associated with subaerial exposure. Stable carbon isotopes are used to quantify meteoric water/rock (W/R) ratios within this cyclic carbonate succession and to investigate the significance of SBs and PSBs. The goals of this contribution are to (1) describe the sequence stratigraphy of the Gobbler Formation, (2) document patterns of stable carbon isotopic variation with respect to SBs and PSBs, (3) develop a mass-balance model to estimate meteoric W/R ratios, and (4) evaluate the relative intensity of meteoric diagenesis in relation to SBs and PSBs.

PALEOGEOGRAPHY AND PALEOCLIMATE

The Gobbler Formation of the Sacramento Mountains and stratigraphic equivalents in the San Andres and Hueco mountains of south-central New Mexico and west Texas (hereafter collectively termed "Gobbler Formation" for brevity) were measured and sampled at meter-scale intervals at eight locales in southern New Mexico and west Texas (Fig. 1; Algeo et al., 1991, 1992). The formation constitutes a 250–450-m-thick

Algeo, T. J., 1996, Meteoric water/rock ratios and the significance of sequence and parasequence boundaries in the Gobbler Formation (Middle Pennsylvanian) of south-central New Mexico, *in* Witzke, B. J., Ludvigson, G. A., and Day, J., eds., Paleozoic Sequence Stratigraphy: Views from the North American Craton: Boulder, Colorado, Geological Society of America Special Paper 306.

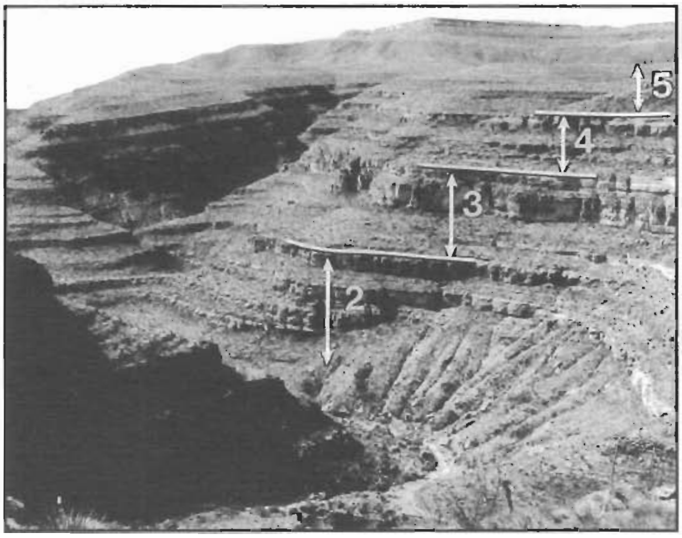

Figure 1. The upper carbonate member of the Gobbler Formation at Bug Scuffle Canyon (southern Sacramento Mountains). Four of five sequences (first not exposed), composed of about 20 parasequences, are visible in 120 m (390 ft) of section.

(820–1,480 ft) succession of shallow-marine sediments of Derryan-Desmoinesian age that is divisible into a lower 75–125-m-thick (250–410 ft) siliciclastic member composed of cross-bedded sandstones, grainy limestones, and shales, and an upper 175–325-m-thick (570–1,070 ft) carbonate member composed of bioturbated micritic limestones and marls ("Bug Scuffle Member" of Pray, 1961). These units, which overlie a Cambrian-Mississippian passive-margin succession, represent the first deposits within the Orogrande Basin, an intracratonic trough that actively subsided during the Pennsylvanian Period owing to crustal stresses associated with the Ouachita-Marathon orogeny (Kottlowski, 1963; Goetz and Dickerson, 1985; Ross and Ross, 1985a). The basin was markedly asymmetric, having a steep, fault-bounded eastern margin (Sacramento Shelf) and a gently inclined western margin (Robledo Ramp; Algeo et al., 1991). The Sacramento Shelf was subject to syndepositional tectonism during the Middle-Late Pennsylvanian resulting from right-lateral transpressional shear within a complex system of regional wrench faulting (Algeo, 1992).

The Orogrande Basin was located at low paleolatitudes, within about 5° of the equator, during the Pennsylvanian Period (Denham and Scotese, 1988). A warm, humid paleoclimate is indicated by the absence of arid-zone features (e.g., dolomite or evaporite, desiccation fabrics, or caliche structures such as nodules, pisoids, and teepees) and by strong meteoric diagenesis of subaerially exposed surfaces in the Gobbler Formation and in overlying units of Late Pennsylvanian age (Goldstein, 1991). Coeval strata in the Paradox, central Colorado, and northern Denver basins to the north, at 10°–20° N paleolatitude, contain extensive evaporite deposits, reflecting their location within an arid climatic belt (Wilson, 1975). However, the Orogrande Basin area was not as humid during the Middle Pennsylvanian as the eastern and mid-continent regions of North America, where moisture-laden trade winds resulted in development of extensive coal swamps (Frakes, 1979).

SEQUENCE STRATIGRAPHY

The carbonate upper member of the Gobbler Formation consists of a succession of 3–20-m-thick (10–66 ft) marl-limestone cycles that are hierarchically arranged in parasequences and sequences (Fig. 1). Individual parasequences are composed of conformable groups of beds and bedsets (terminology of Sarg, 1988; Van Wagoner et al., 1990), each of which is relatively homogeneous internally and is separated from adjacent beds and bedsets of similar lithology by distinct bedding surfaces (Fig. 2). Parasequences exhibit strong asymmetry, being composed of generally thin (<1–2 m [3.3–6.6 ft]) recessive bases and thick (3–20 m [10–66 ft]) resistant caps. Recessive basal units mainly consist of nodular marls, locally containing abundant sponge spicules. Resistant caps are largely composed of fossil wackestone and packstone containing an abundant, diverse open-marine biota, including echinoderms, bryozoans, brachiopods, phylloid algae, fusulinids, endothyrids, tubular foraminifera, rugose and tabulate corals, *Komia* (a small dendroid stromatoporoid), and *Chaetetes* (a sponge-like organism of uncertain affinity; Wilson, 1975). In more proximal areas, some parasequences are capped by cross-bedded fossiliferous or oolitic grainstone. Each parasequence is interpreted to represent a single transgressive-regressive sea-level cycle, in which the maximum flooding surface (MFS) is located within the recessive basal unit and the overlying resistant beds and bedsets represent deposition under conditions of stable or falling sea level.

The tops of individual parasequences are marked by sharp, disconformable surfaces exhibiting brecciated rubble (generally of the same lithology as the underlying rock and of parautochthonous origin), black pebble conglomerates, karst solution pits and rills (rillenkarren), and sandy laminar or ferric oxidized crusts (Fig. 2; Algeo et al., 1991). Directly overlying many cycle tops are thin (1–10 cm [0.4–4 in]) layers of coarse-grained, echinoderm-rich fossil debris containing abundant phosphatic grains, glauconite pellets, and quartz sand. Irregular small-scale relief (<1 m [3.3 ft]) is developed along the upper surface of some parasequences. Collectively, these features document subaerial exposure of parasequence tops and deposition of winnowed lags during subsequent transgressions, suggesting that these surfaces are type 1 unconformities (Sarg, 1988).

Sequences consist of groups of four to six parasequences and range in thickness from 30 to 70 m (100–230 ft) (Fig. 3). They exhibit moderate to strong asymmetry owing to the decreased shale content and increased weathering resistance of component parasequences at stratigraphically higher levels. Within each sequence, parasequences become coarser grained and cleaner upward, developing caps composed of skeletal packstone or grainstone. This asymmetry permits ready field recognition of parasequence-sequence hierarchies at most study locales

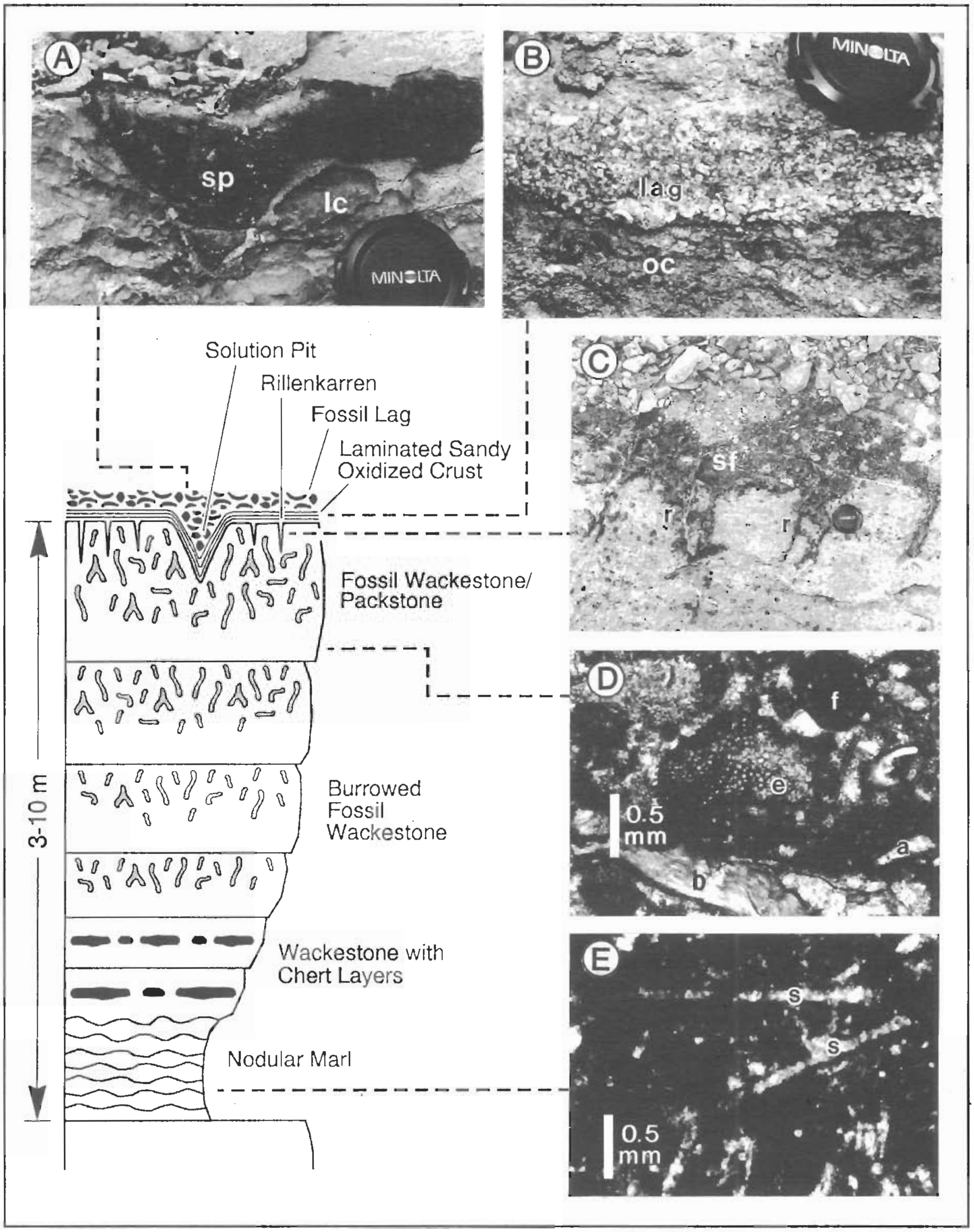

Figure 2. Lithologies and diagenetic features of Gobbler Formation parasequences. Parasequence tops exhibit a variety of features associated with subaerial exposure and meteoric diagenesis: (A) karst solution pit (sp), lined by sandy laminar crust (lc) and infilled by silicified fossil lag; (B) coarse-grained fossil lag overlying platy oxidation crust (oc) at parasequence boundary; and (C) rillenkarren (r) developed on cycle-top exposure surface (sf) and accentuated by later silicification. Major lithologies include (D) fossil wackestones with abundant echinoderms (e), fusulinids (f), phylloid algae (a), and brachiopods (b), and (E) argillaceous wackestones containing abundant sponge spicules (s).

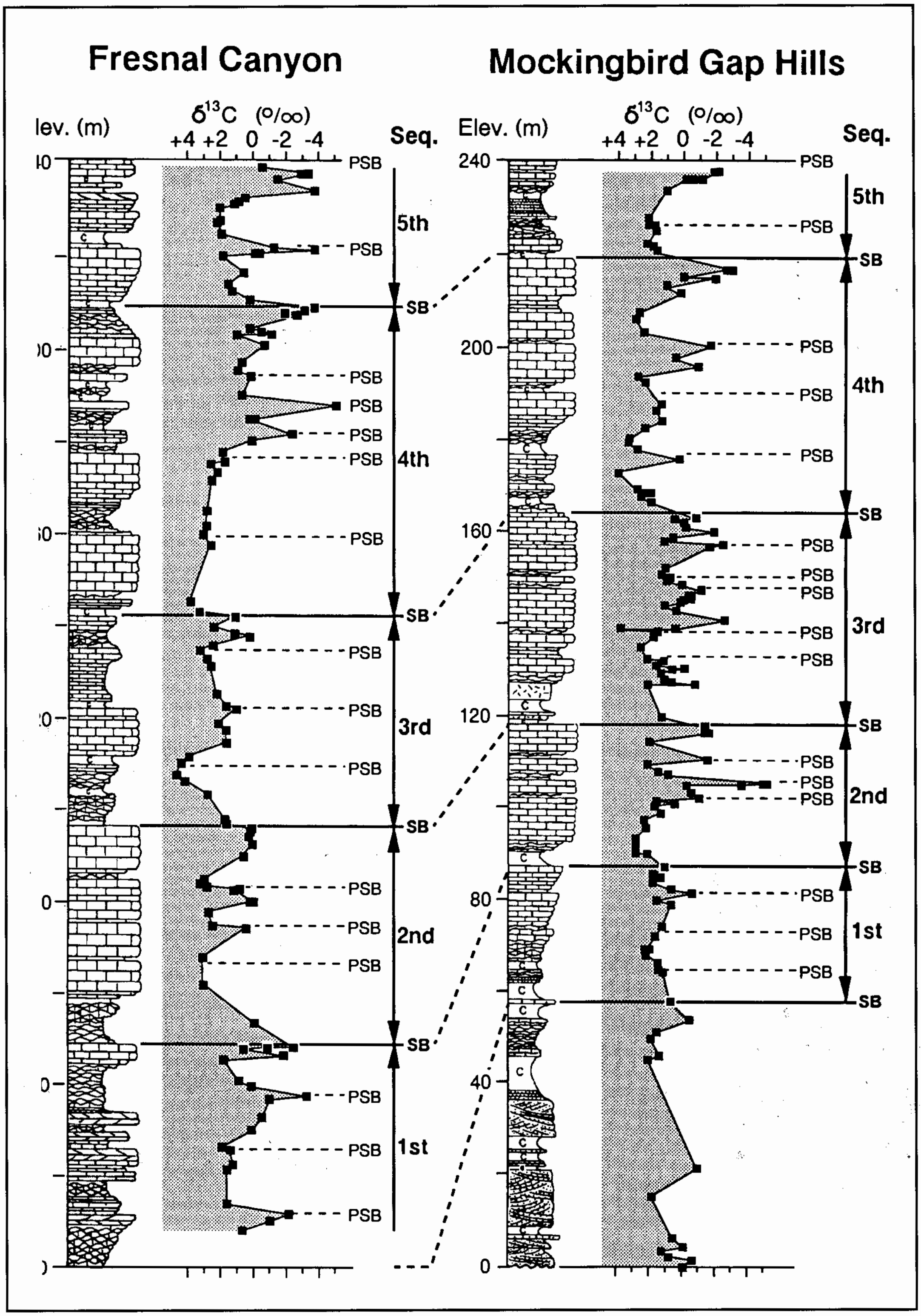

Figure 3. Stratigraphic columns and micrite carbon isotope stratigraphies of the Fresnal Canyon and Mockingbird Gap Hills sections. Sequences are numbered 1–5, SB = sequence boundary, PSB = parasequence boundary, c = covered interval. Note the relation between micrite ^{13}C depletion and sequence and parasequence boundaries. The base of the Fresnal Canyon section is incomplete owing to nonexposure.

marine-carbonate baseline established from articulate brachiopods. The following discussion is based on about 400 stable carbon and oxygen isotopic analyses of Gobbler Formation micrites and 9 analyses of brachiopod shell material (all values given in parts per mille Peedee belemnite; see Algeo et al., 1992, for a description of isotopic methods). Two sections, Mockingbird Gap Hills and Fresnal Canyon, were chosen for in-depth isotopic analysis (n = 123 and 108, respectively). These sections represent the most proximal locales on the western and eastern margins of the Orogrande Basin, respectively, and were regarded as likely areas of strong meteoric diagenesis in the event of large-scale sea-level fluctuations.

Micrite $\delta^{13}C$ Variation

The carbon isotopic compositions of Gobbler Formation micrites range from +5.0‰ to –5.8‰ and exhibit high-frequency variation closely associated with parasequence boundaries (Fig. 3). The uppermost few meters of many parasequences are characterized by large negative $\delta^{13}C$ excursions with progressively heavier $\delta^{13}C$ values stratigraphically downward within the unit. Generally, a sharp transition exists between ^{13}C-depleted values at the top of one parasequence and ^{13}C-enriched values at the base of the next parasequence. Few ^{13}C-depleted values occur more than 1–2 m (3.3–6.6 ft) below PSBs.

The association of ^{13}C-depleted cements with subaerial exposure surfaces is common in both ancient and modern carbonates (e.g., Allan and Matthews, 1982; Brown, 1982; Beier, 1987; Budd and Land, 1990; Goldstein, 1991; Saller and Moore, 1991). Depleted carbon isotopic signatures result from early meteoric diagenesis of the exposed limestone surfaces. Meteoric fluid laden with ^{12}C derived from soil-zone organics fluxes downward and mixes with isotopically heavy carbonate carbon derived from host-rock dissolution. Owing to a progressive increase in fluid-rock interaction downward, meteoric cements precipitated at depth have a lower proportion of fluid-derived carbon than those precipitated close to an exposure surface. The absence of negative carbon isotopic excursions along some Gobbler Formation parasequence tops (Fig. 3) probably reflects control of fluid flow by local rock-matrix heterogeneities (Algeo et al., 1992). Petrographic evidence of subaerial exposure (e.g., Fig. 2) is generally strongest for those parasequence caps exhibiting large negative $\delta^{13}C$ excursions, consistent with variation in fluid flux and in the degree of meteoric alteration from one parasequence to the next.

Micrite $\delta^{18}O$ Variation

Gobbler Formation micrites have oxygen isotopic compositions ranging from less than –14‰ to –2.9‰ (Fig. 4). Each section exhibits a characteristic mean $\delta^{18}O$ value, ranging from a low of –10.5‰ at Hembrillo Canyon to a high of –4.3‰ at Fresnal Canyon (at –6.9‰, Mockingbird Gap Hills is intermediate). Strong correlation between section-average $\delta^{18}O$ values

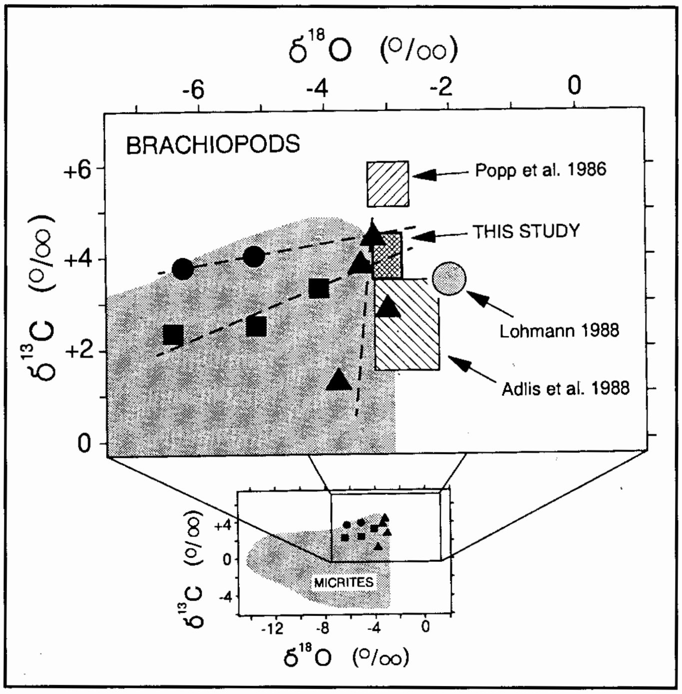

Figure 4. Primary marine-carbonate isotopic compositions. Well-preserved articulate brachiopods (symbols) exhibit more limited isotopic variation than matrix micrites (shaded area). Analyses of multiple samples from individual sections exhibit carbon-oxygen covariance: Mockingbird Gap Hills samples (squares), Fresnal Canyon (triangles), and Hembrillo Canyon (circles). The intersection of these trends (dashed lines) represents the probable isotopic composition of unaltered primary marine carbonate: +4.0 ± 0.5 $\delta^{13}C$ and –3.0 ± 0.2 $\delta^{18}O$ (cross-hatched block). Isotopic depletion of brachiopods relative to primary marine carbonate is probably due to precipitation of cements within shell micropores.

and maximum burial depths at a given locale indicate dominant control of oxygen isotopic compositions by burial temperature (Algeo et al., 1992). Micrite $\delta^{18}O$ values exhibit no relation to PSBs or SBs. Despite significant shifts in micrite $\delta^{18}O$ values during burial diagenesis, carbon isotopic values were largely unaffected owing to low fluid C concentrations and low W/R ratios in the burial diagenetic environment (Algeo et al., 1992). Burial diagenesis resulted in slight homogenization of carbon isotopes (i.e., minor reduction of the range of micrite $\delta^{13}C$ values) with progressive ^{18}O depletion (Fig. 4).

Marine-carbonate isotopic composition

In order to evaluate the degree of meteoric alteration of Gobbler Formation micrites, it is necessary to establish a primary marine-carbonate $\delta^{13}C$ baseline. First, because most diagenetic processes result in depletion of ^{13}C and ^{18}O in secondary precipitates relative to primary marine carbonates (e.g., Meyers and Lohmann, 1985), the isotopically heaviest micrite compositions may approximate such a baseline. The most-enriched isotopic values exhibited by Gobbler Formation micrites are +5.0‰ $\delta^{13}C$

(although only a few samples are heavier than +4.0‰) and –2.9‰ $\delta^{18}O$ (Fig. 4; Algeo et al., 1992). Second, owing to their stable low-Mg calcite mineralogy, articulate brachiopods with well-preserved shell microstructure (as verified by cathodoluminescence petrography) generally yield good estimates of primary marine-carbonate isotopic composition (Lowenstam, 1961; Popp et al., 1986; Veizer et al., 1986; Adlis et al., 1988). Gobbler Formation brachiopods, although exhibiting some variation in carbon and oxygen isotopic values, are always isotopically enriched relative to cosampled micrites. Multiple analyses from individual sections exhibit carbon-oxygen covariance, yielding linear arrays of values that converge at ~+4.0‰ $\delta^{13}C$ and –3.0‰ $\delta^{18}O$ (Fig. 4). On the basis of these considerations, the isotopic composition of Middle Pennsylvanian marine carbonates is estimated to be +4.0‰ ± 0.5‰ $\delta^{13}C$ and –3.0 ± 0.2‰ $\delta^{18}O$. These values are in good agreement with previous estimates of Pennsylvanian marine-carbonate isotopic compositions by Popp et al. (1986), Lohmann (1988), and Adlis et al. (1988; Fig. 4).

Isotopic mass balance modeling of meteoric water/rock ratios

The isotopic composition of any diagenetic phase is a function of initial pore-fluid and host-rock isotopic compositions, the relative molar contribution of each source, and the fractionation factor between a precipitate and coexisting fluid at equilibrium. The relative molar contributions of the fluid and rock sources determine the molar W/R ratio, which can be related to volumetric W/R ratio via the relative concentration of the element of interest in the fluid and rock sources. Water/rock ratios calculated on either basis record only the amount of pore fluid which has moved through *and* reacted with the host rock. The carbon isotopic composition of a meteoric diagenetic precipitate can be related to W/R ratio through a simple mass balance model, in which the isotopic composition of the precipitate equals a mole-weighted average of the isotopic compositions of the pore fluid and host rock:

$$\delta_p = \left(M_f \left(\delta_f + \varepsilon_{HCO_3^-(aq)}^{CaCO_3(s)} \right) + M_r \delta_r \right) / \left(M_f + M_r \right) \qquad (1)$$

where δ_p = $\delta^{13}C$ of diagenetic precipitate, δ_f = initial $\delta^{13}C$ of pore fluid, δ_r = initial $\delta^{13}C$ of host carbonate, M_f = molar contribution of carbon from pore fluid, M_r = molar contribution of carbon from host carbonate, and $\varepsilon_{CaCO_3(s)/HCO_3^-(aq)}$ = carbon isotopic fractionation between aqueous bicarbonate and meteoric calcite expressed in per-mil variation.

Carbon isotopic values of meteoric precipitates reflect the degree of openness of the diagenetic system through $\varepsilon_{CaCO_3(s)/HCO_3^-(aq)}$. In an open system (i.e., with unlimited fluid supply), M_f is much larger than M_r, and maximum calcite-bicarbonate fractionation occurs (+1.0 ± 0.2‰; Romanek et al., 1992). In a closed system (i.e., with minimal fluid and no replenishment), M_r is large in relation to M_f, and calcite-bicarbonate fractionation is reduced owing to Rayleigh fractionation of carbon isotopes within the limited volume of available fluid. Equation 1 may be reorganized to solve directly for molar W/R ratio:

$$M_f / M_r = \left(\delta_r - \delta_p \right) / \left(\delta_p - \delta_f - \varepsilon_{HCO_3^-(aq)}^{CaCO_3(s)} \right) \qquad (2)$$

Molar W/R ratio can be converted to volumetric W/R ratio by a constant κ:

$$V_f / V_r = \left(M_f / M_r \right) \kappa, \qquad (3)$$

where V_f/V_r is the volumetric W/R ratio. Reorganizing to solve for κ yields:

$$\kappa = \left(M_r / V_r \right) / \left(M_f / V_f \right), \qquad (4)$$

where M_r / V_r = moles of carbon per unit volume of rock, and M_f / V_f = moles of carbon per unit volume of fluid, and:

$$M_r / V_r = 10^6 C_{CaCO_3} \rho_{CaCO_3} / w_c, \qquad (5)$$

where C_{CaCO_3} = concentration of carbon in calcite by weight (12 g C/100 g $CaCO_3$), r_{CaCO_3} = density of calcite (2.7 g/cm³), w_C = molecular weight of carbon (12 g/mol), and 10^6 is a unit-conversion factor. Given these values, $\kappa = 2.7 \times 10^4/TIC$ (equation 4), where TIC = concentration of total inorganic carbon in the fluid in mmol/l. Rearranging equations 2 and 3 and substituting for κ yields:

$$V_f / V_r = \left(2.7 \cdot 10^4 / TIC \right) \left(\delta_r - \delta_p \right) / \left(\delta_p - \delta_f - \varepsilon_{HCO_3^-(aq)}^{CaCO_3(s)} \right) \qquad (6)$$

All subsequent discussion of meteoric W/R ratios will be on a volumetric rather than a molar basis.

Initial parameters for meteoric water/rock ratio model

In order to calculate model meteoric W/R ratios based on equation 6, values are required for four parameters: (1) meteoric precipitate $\delta^{13}C$, (2) primary marine-carbonate $\delta^{13}C$, (3) initial meteoric fluid $\delta^{13}C$, and (4) fluid total inorganic carbon (TIC) concentration. The first two variables can be constrained by direct isotopic analysis of carbonate components within the Gobbler Formation. The carbon isotopic compositions of Gobbler Formation micrites were set within the meteoric environment and altered little within the burial environment (Algeo et al., 1992); thus, meteoric precipitate $\delta^{13}C$ is measured directly from matrix micrites (Fig. 3). As discussed above, the carbon isotopic composition of primary marine carbonate can be estimated from isotopically heavy micrites and well-preserved articulate brachiopods, and is ~+4.0‰ ± 0.5‰ (Fig. 4).

The $\delta^{13}C$ value and TIC concentration of the initial meteoric fluid can be estimated based on the composition of soil solutions in comparable modern climate zones. The immediate source of soil carbon is terrestrial vegetation, and both modern and ancient land plants using the C3 photosynthetic pathway exhibit limited $\delta^{13}C$ variation (ca. –26‰ ± 1‰; Degens, 1969; Deines, 1980; Popp et al., 1989). Although plants using the C4 and CAM photosynthetic pathways are isotopically enriched by comparison (ca. –6‰ to –19‰ and –12‰ to –23‰, respectively), they probably did not exist in the pre-Cenozoic (Cerling et al., 1993; Morgan et al., 1994). Thus, Pennsylvanian soil organic carbon is likely to have been sourced entirely from C3 vegetation.

In addition to vegetation type, the $\delta^{13}C$ values of soil CO_2 can be influenced by such factors as atmospheric pCO_2, soil respiration rate, porosity, and temperature (Cerling, 1991). Although atmospheric pCO_2 during the late Paleozoic is not known with any degree of certainty, values were probably relatively low (ca. 0.5–1.0 PAL; Berner, 1991, 1994) as a result of rapid burial of organic carbon during Late Devonian–Early Carboniferous time. At low values of atmospheric pCO_2, little, if any, atmospheric CO_2 ($\delta^{13}C$ = –6.5‰) diffuses downward into soils, and soil respiration rate and porosity have little effect on the isotopic composition of soil gas (Cerling, 1991).

Temperature is of moderate importance in determining the carbon isotopic composition of soil solutions owing to fractionation between soil gas and dissolved bicarbonate (Cerling, 1991). For temperatures in the range of 10–40°C, $HCO_3^-(aq)$–$CO_2(g)$ fractionation is approximately:

$$\varepsilon_{CO_2(g)}^{HCO_3^-(aq)} = +11.0(\pm 0.3) - 0.12(\pm 0.01)T, \qquad (7)$$

where T is temperature in °C (Romanek et al., 1992). In addition, a +4.4‰ enrichment of $CO_2(g)$ relative to C_{org} occurs in soils owing to faster diffusion of ^{12}C versus ^{13}C outward to the atmosphere. Thus, the carbon isotopic composition of dissolved bicarbonate in Pennsylvanian soil solutions was approximately:

$$\delta_b = -26 \pm 1 + 4.4 + 11.0(\pm 0.3) - 0.12(\pm 0.01)T, \qquad (8)$$

where δ_b is the $\delta^{13}C$ value of dissolved soil bicarbonate. Equatorial temperatures are thought to have been relatively constant throughout the Phanerozoic despite large-scale global climate changes (Frakes, 1979). For modeling purposes, a mean annual temperature of 25 ± 5°C (a range consistent with an equatorial coastal setting) is assumed, yielding $HCO_3^-(aq)$–$CO_2(g)$ fractionation of +8.0‰ ± 1.1‰ (equation 7) and a $\delta^{13}C$ value for dissolved bicarbonate in humid, low-latitude Pennsylvanian soils of –13.5‰ ± 2‰ (equation 8).

The final model parameter, the initial TIC concentration of meteoric fluids, can be estimated based on the composition of modern soil solutions in climatically comparable environments. In modern temperate- to tropical-zone soils developed on calcareous host rock ("brown forest soils"), bicarbonate forms in the uppermost (A) horizons through solution and dissociation of oxidized organic carbon. Dissolved bicarbonate concentrations in such soils are consistently rather high, ca. 700–1000 mg/l (Matthess, 1982), which is equivalent to a bicarbonate molar concentration of 12 ± 2 mmol/l. Bicarbonate represents by far the largest component of total inorganic carbon in such systems and is a good proxy for TIC.

In summary, the parameters used in calculating model meteoric W/R ratios for the Gobbler Formation via equation 6 are (sources in parentheses): δ_p = measured $\delta^{13}C$ in ‰ (Gobbler Formation micrites); δ_r = +4.0‰ ± 0.5‰ (Gobbler Formation brachiopods); δ_f = –13.5‰ ± 2‰ (calculated assuming C3 vegetation); $\varepsilon_{CaCO_3(s)/HCO_3^-(aq)}$ = +1.0‰ ± 0.2‰ (experimentally determined; Romanek et al., 1992); TIC = 12 ± 2 mmol/l (estimated based on modern temperate zone soil waters; Matthess, 1982).

Variability of meteoric water/rock ratios within parasequences

Within individual parasequences, micrites generally exhibit ^{13}C enrichment downsection, indicating smaller contributions of isotopically light soil-derived carbon at depth (Fig. 5). Assuming that Gobbler Formation micrites initially had an average isotopic composition equal to that of primary marine carbonate ($\delta^{13}C$ = +4.0‰ ± 0.5‰), their present degree of ^{13}C depletion provides a measure of the relative molar contribution of carbon from fluid and rock sources and, thus, of meteoric W/R ratio. Differences in the degree of micrite ^{13}C depletion in successive parasequence caps probably reflect variation in meteoric fluid flux across these surfaces, although variable development of overlying soil horizons may have played a role. Differences in the rate of micrite ^{13}C enrichment downsection within parasequences reflect a combination of variable meteoric fluid volume and host-rock susceptibility to diagenetic reaction. Thus, although a number of factors contributed to changes in micrite $\delta^{13}C$ with depth below parasequence tops, these can be usefully summarized as "meteoric W/R ratio," providing a quantitative measure for comparison of meteoric effects among parasequences.

Changes in meteoric W/R ratios downward within individual parasequences can be calculated based on the isotopic mass balance model developed above and documented patterns of downsection enrichment of micrite carbon isotopes. The latter parameter was determined as a weighted running average of micrite $\delta^{13}C$ values with respect to depth below PSBs. At Mockingbird Gap Hills, micrite $\delta^{13}C$ values increase, on average, from –0.4‰ at parasequence boundaries to +2.4‰ at a depth of 10 m (33 ft) (Fig. 5). This rate of ^{13}C enrichment is comparable in magnitude to that reported for several Quaternary limestone units (e.g., Beier, 1987; Budd and Land, 1990). Average meteoric W/R ratios calculated from this trend range from about 800 at parasequence tops to about 200 at 10 m (33 ft) depth (Fig. 5; equation 6). Compounded uncertainties in the various model parameters permit parasequence-cap W/R ratios potentially to be as high as 1500 or as low as 450, and those at 10 m (33 ft) depth to be as high as 500 or as low as 80. All combinations of model values yield relatively high W/R ratios, indicating that meteoric diagenesis proceeded within a largely open system.

Meteoric W/R ratios decrease downsection over a 10 m (33 ft) interval by a factor of three to six (Fig. 5). Such downsection decrease is a result of two processes operating within Gobbler Formation meteoric systems. First, lateral diversion of

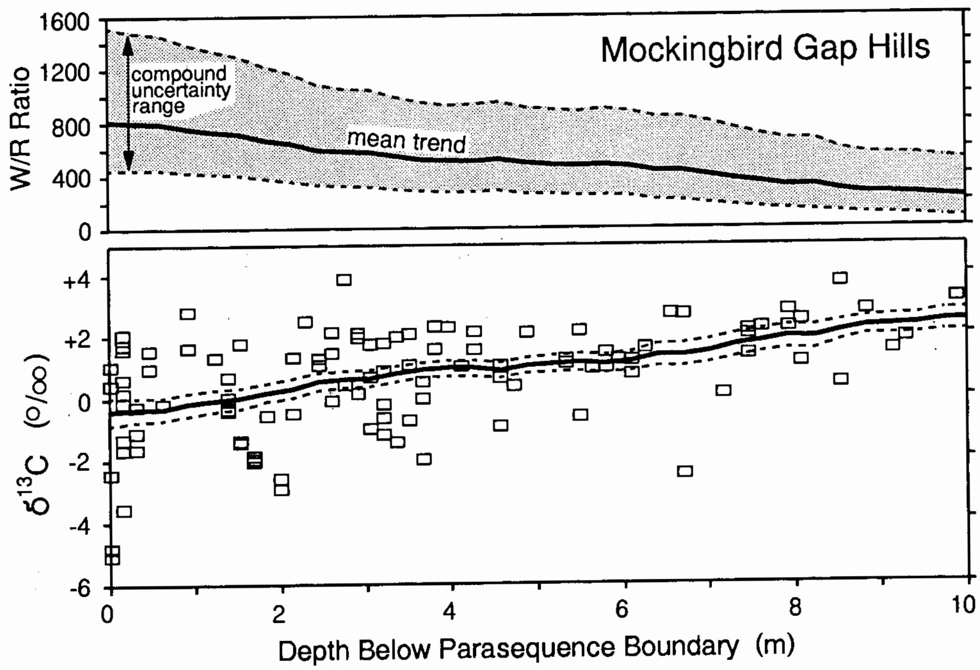

Figure 5. Model meteoric water/rock ratios with respect to parasequence boundaries at Mockingbird Gap Hills. The model utilizes depth-dependent micrite $\delta^{13}C$ values based on a weighted running average (solid line, bottom), marine carbonate $\delta^{13}C$ = +4.0 ± 0.5‰, meteoric fluid $\delta^{13}C$ = −13.5 ± 2‰, $\varepsilon_{CaCO_3/HCO_3^-}$ = +1.0 ± 0.2‰, and fluid TIC (total inorganic carbon) concentration = 12 ± 2 mmol/l. Resulting volumetric estimates of meteoric W/R ratios range from 800 at parasequence caps to 200 at a depth of 10 m (solid line, top). Uncertainty limits for meteoric W/R ratio estimates (dashed lines, top) were calculated as compounded uncertainty ranges of all model parameters, including ±1 standard mean error for the weighted $\delta^{13}C$ running average (dashed lines, bottom). A similar range of meteoric W/R ratios was calculated for Fresnal Canyon (not shown).

meteoric fluids occurred owing to vertical permeability barriers (especially marly units at parasequence bases), causing an *actual* decrease in meteoric W/R ratios. Second, progressive reaction of meteoric fluids with host carbonate resulted in evolution of the fluid carbon isotopic composition at depth toward heavier marine-carbonate values and an accompanying *apparent* decrease in meteoric W/R ratio. As the relative importance of these processes is unknown, reported meteoric W/R ratios are understood to include both. A further potential complication is that, owing to the large amplitude of Middle Pennsylvanian sea-level changes (e.g., Crowley and Baum, 1991), meteoric lenses of successive lowstands may have overlapped. This would have resulted in multiple stages of meteoric alteration of a single parasequence, although a three- to six-fold reduction in meteoric W/R ratios over each 10 m (33 ft) interval downsection (e.g., Fig. 5) would have attenuated the effects of diagenetic overprints by later meteoric lenses.

Significance of sequence versus parasequence boundaries

Within most Gobbler Formation sequences, the lowermost parasequence has a thick marly base and stratigraphically higher parasequences exhibit increased graininess and reduced micrite content, indicating progressively shallower water conditions (Fig. 3). Facies stacking patterns of this type are commonly simulated using a sea-level forcing function modeled by two sine waves of differing periods and amplitudes (e.g., Goldhammer et al., 1991; Read et al., 1991). If formation of sequences and parasequences reflects such a forcing mechanism, this should be manifested in systematic variation in the degree of exposure of PSBs within sequences. In this scenario, high-frequency sea-level falls exhibit reduced amplitude during intervals of rising long-term sea level, but increased amplitude during intervals of falling long-term sea level (e.g., Osleger and Read, 1991, fig. 15). Thus, parasequence tops at the base of a sequence should undergo shorter intervals of exposure than those at the top of a sequence and, hence, should exhibit less intense meteoric alteration.

Meteoric carbonate carbon isotopes provide a means of quantitatively testing this hypothesis. Because longer or more intense meteoric alteration should be reflected in greater overall ^{13}C depletion toward a given exposure surface, the distribution of meteoric carbonate $\delta^{13}C$ values with respect to SBs and PSBs (e.g., Fig. 3) may provide information on the relative intensity of meteoric diagenesis undergone at these surfaces. If the rate of sea-level change of long-period cycles is small relative to that of short-period cycles ($A_1/\lambda_1 << A_2/\lambda_2$), then all parasequences (including those capping sequences) should undergo similar degrees of meteoric alteration and isotopic depletion (e.g., dashed lines, Fig. 6A). In this case, micrite $\delta^{13}C$ values should exhibit a strong relation to PSBs (dashed line, Fig. 6B) but only a weak relation to SBs (dashed line, Fig. 6C). Conversely, if the rate of sea-level change of long-period cycles is large relative to that of short-period cycles ($A_1/\lambda_1 >> A_2/\lambda_2$), then SBs should undergo more intense meteoric alteration than PSBs (e.g., solid lines, Fig. 6A), and micrite $\delta^{13}C$ values should exhibit a stronger relation to the former (solid line, Fig. 6C) than to the latter (solid line, Fig. 6B).

The strength of these relations can be evaluated based on correlation coefficients (r^2), which represent the amount of variance accounted for through linear regression of a dataset. If the r^2 value for micrite $\delta^{13}C$ versus depth below SBs is smaller than that versus depth below PSBs (e.g., Fig. 6B), then the former surfaces are equivalent to the latter with regard to intensity of meteoric diagenesis. Conversely, if the r^2 value for SBs is larger than that for PSBs (e.g., Fig. 6C), then micrite ^{13}C depletion is mainly controlled by diagenesis at SBs, and these surfaces are likely to have undergone longer or more intense exposure than the "average" PSB. A correlation coefficient approaching 1.0 would indicate strong control of meteoric carbonate $\delta^{13}C$ values by PSBs or SBs, whereas a value approaching 0 would indicate no control by the respective boundary type. Weak correlation of meteoric carbonate $\delta^{13}C$ values with SBs or PSBs may reflect an incidental relation resulting from strong control by the other boundary type. For example, if diagenetic alteration were associated exclusively with SBs ($r^2 = 1.0$), $\delta^{13}C$ values versus depth below PSBs would nonetheless yield r^2 equal to $1/n^2$ (where n is the number of parasequences per sequence; in Fig. 6, $n = 3$ and $r^2 = 0.11$; for the Gobbler Formation, $n = 4$–6 and $r^2 \approx 0.03$–0.06).

Gobbler Formation micrites exhibit ^{13}C depletion with respect to both PSBs and SBs (Fig. 7). In the Fresnal Canyon section, micrite ^{13}C depletion trends are weak in relation to both types of boundaries ($r^2 = 0.07$–0.09). Because many exposure surfaces in the Fresnal Canyon section exhibit ^{13}C depletion (Fig. 3), low r^2 values appear to reflect a high degree of isotopic scatter about the mean depth trend (Fig. 7, top). This suggests that patterns of meteoric fluid flow in the Fresnal Canyon section were affected by large heterogeneities in matrix permeability, or possibly the effects of multiple diagenetic overprints. In contrast, the depth dependency of micrite $\delta^{13}C$ values is greater for both boundary types in the Mockingbird Gap Hills section, in which micrite ^{13}C depletion correlates more strongly with SBs ($r^2 = 0.25$) than PSBs ($r^2 = 0.18$; Fig. 7, bottom). These results indicate moderately strong control of meteoric diagenesis by exposure surfaces and longer or more intense alteration of SBs than PSBs.

Differences in ^{13}C depletion trends between the two study locales may reflect regionally variable tectonic and sedimentation patterns within the Orogrande Basin. The Mockingbird Gap Hills section was located on the stable western basin margin (Robledo Ramp), yielding regular facies stacking patterns

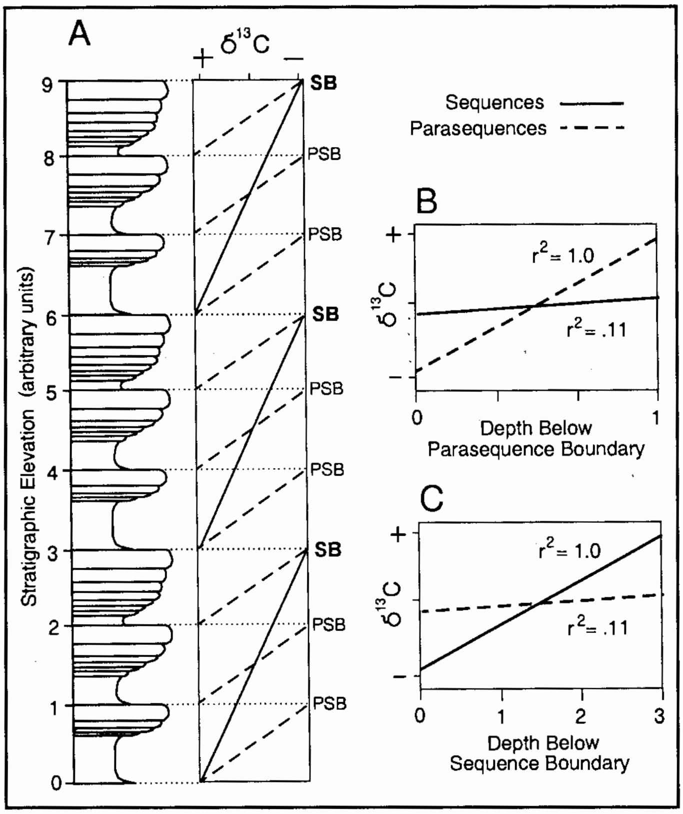

Figure 6. Model ^{13}C depletion patterns and associated correlation coefficients in a section composed of three sequences and nine parasequences (A). Sequence boundaries (SB) and parasequence boundaries (PSB) shown at right. If meteoric carbonate carbon isotopes are controlled by diagenesis at PSBs (dashed lines), then $\delta^{13}C$ values should correlate strongly with depth below PSBs (B) and only weakly with depth below SBs (C). Conversely, if meteoric isotopes are controlled by diagenesis at SBs (solid lines), then $\delta^{13}C$ values should correlate strongly with depth below SBs (C) and only weakly with depth below PSBs (B). The first case implies that SBs and PSBs underwent equivalent degrees of meteoric alteration, whereas the second case implies stronger alteration of SBs than PSBs.

(Fig. 3) and control of meteoric diagenesis by quasiperiodic sea-level changes. Conversely, the Fresnal Canyon section was located on the tectonically active eastern basin margin (Sacramento Shelf), resulting in less-regular facies stacking patterns and, probably, more heterogeneous matrix permeabilities that influenced vertical and lateral fluid migration within meteoric lenses. Facies control of meteoric fluid flow, rather than vertical motions of the shelf per se, are more likely to have produced the weak relation of micrite $\delta^{13}C$ values to SBs and PSBs in the Fresnal Canyon section (Fig. 7).

CONCLUSIONS

1. The upper carbonate member of the Middle Pennsylvanian Gobbler Formation of south-central New Mexico is composed of 3–20-m-thick (10–66 ft) parasequences capped by

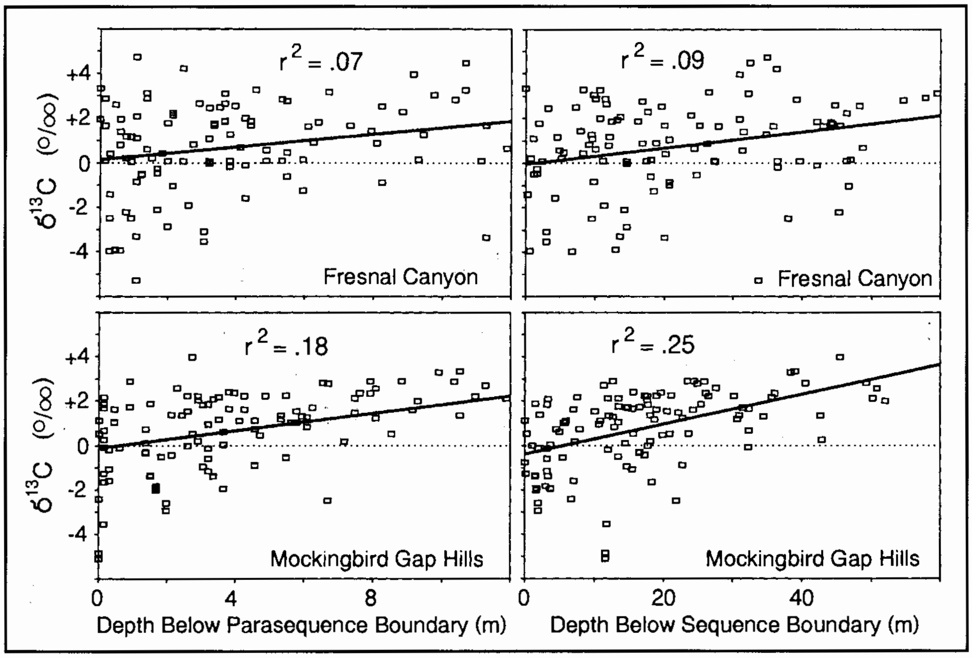

Figure 7. Micrite ^{13}C depletion patterns with respect to sequence boundaries (SB) and parasequence boundaries (PSB) in the Fresnal Canyon and Mockingbird Gap Hills sections. Note that carbon isotopic depletion is greater by 2‰ to 4‰ at the tops of sequences and parasequences than at their bases. SBs and PSBs exert weak control on micrite $\delta^{13}C$ values at Fresnal Canyon ($r^2 = 0.07$–0.09; not significant at the 5% confidence level) and moderate control at Mockingbird Gap Hills (PSB $r^2 = 0.18$, $\alpha \leq 5\%$; SB $r^2 = 0.25$, $\alpha \leq 1\%$, d.f. = 121, Snedecor and Cochran, 1967). At Mockingbird Gap Hills, SBs apparently represent exposure surfaces subjected to longer or more intense meteoric diagenesis than PSBs.

sharp, disconformable surfaces exhibiting petrographic and isotopic evidence of subaerial exposure and meteoric diagenesis.

2. Groups of four to six parasequences comprise individual 30–70-m-thick (100–230 ft) sequences. Within each sequence, individual parasequences become less shaly and coarser-grained upsection, and parasequence caps tend to exhibit stronger development of subaerial exposure features and greater ^{13}C depletion of meteoric carbonates.

3. Gobbler Formation parasequences are widely correlatable (>100 km [62 mi]) laterally across the Orogrande Basin, show evidence of early meteoric diagenesis in both shelf and basinal areas, exhibit strong modal thicknesses at each locale, and represent an average depositional period of ca. 120–180 ka. The most likely mechanism to produce such regular, large-amplitude, high-frequency changes of relative sea level over substantial lateral distances is glacio-eustasy.

4. Well-preserved articulate brachiopods and isotopically heavy micrites indicate a primary marine-carbonate isotopic composition of +4.0‰ ± 0.5‰ $\delta^{13}C$ and −3.0‰ ± 0.2‰ $\delta^{18}O$ for the Gobbler Formation.

5. Isotopic patterns document two stages of diagenesis within the Gobbler Formation: an early meteoric phase associated with episodic subaerial exposure that largely controlled micrite $\delta^{13}C$ values, and a later burial phase that reset micrite $\delta^{18}O$ values without substantially altering carbon isotopic ratios.

6. Micrite $\delta^{13}C$ values range from +5.0‰ to −5.8‰ and exhibit high-frequency variation closely associated with exposure surfaces, in which the uppermost few meters of many parasequences are characterized by large negative $\delta^{13}C$ excursions.

7. Meteoric precipitates record mixing of carbon from isotopically heavy marine carbonate ($\delta^{13}C$ = +4.0‰ ± 0.5‰) and isotopically light, soil-derived meteoric bicarbonate ($\delta^{13}C$ = −13.5‰ ± 2‰) sources.

8. Mass-balance modeling indicates that meteoric diagenesis took place within a largely open system, in which meteoric W/R ratios decreased from about 800 at parasequence tops (uncertainty limits 450–1500) to about 200 at 10 m (33 ft) depth (uncertainty limits 80–500). A three- to six-fold decrease in W/R ratio at 10 m (33 ft) intervals downsection indicates strong evolution of fluid isotopic compositions and/or substantial lateral flow owing to vertical permeability barriers.

9. In the Mockingbird Gap Hills section, micrite ^{13}C depletion is stronger with respect to sequence boundaries than parasequence boundaries (r^2 = 0.25 versus 0.18), implying that the former/present exposure surfaces of greater duration and/or diagenetic intensity than the latter. Sequence and parasequence

boundaries exert only weak control on micrite $\delta^{13}C$ values in the Fresnal Canyon section ($r^2 = 0.07–0.09$).

ACKNOWLEDGMENTS

This manuscript benefitted from reviews by Maya Elrick, Philip Heckel, and Greg Ludvigson, and constructive criticisms of an earlier version were provided by Linda Albertzart, Steve Dorobek, Terry Quinn, Lynn Walter, and Donald Zenger. I thank Lyla Messick and Lisa Trump for drafting services, the U.S. Army for permission to conduct field work within the White Sands Missile Range, and Max Canestorp for assistance while on base. This study was supported by a National Science Foundation Graduate Fellowship and the University of Michigan Scott Turner Fund. I gratefully acknowledge the guidance of Bruce Wilkinson and Kyger Lohmann in completing the dissertation from which most of this study is drawn. Isotopic analyses were performed in the Stable Isotope Laboratory at the University of Michigan.

REFERENCES CITED

Adlis, D. S., Grossman, E. L., Yancey, T. E., and McLerran, R. D., 1988, Isotope stratigraphy and paleodepth changes of Pennsylvanian cyclical sedimentary deposits: Palaios, v. 3, p. 487–506.

Algeo, T. J., 1992, Continent-scale wrenching of southwestern Laurussia during the Ouachita-Marathon Orogeny and tectonic escape of the Llano block, *in* Lindsay, R. F., and Reed, C. L., eds., Sequence stratigraphy applied to Permian Basin reservoirs: Outcrop analogs in the Caballo and Sacramento mountains of New Mexico: Midland, Texas, West Texas Geological Society, p. 115–131.

Algeo, T. J., Wilson, J. L., and Lohmann, K. C, 1991, Eustatic and tectonic controls on cyclic sediment accumulation patterns in Lower-Middle Pennsylvanian strata of the Orogrande Basin, New Mexico, *in* Barker, J. M., Kues, B. S., and Austin, G. S., eds., Geology of the Sierra Blanca and Capitan ranges, New Mexico: New Mexico Geological Society, 42nd Annual Field Conference, Guidebook, p. 203–212.

Algeo, T. J., Wilkinson, B. H., and Lohmann, K. C, 1992, Meteoric-burial diagenesis of Middle Pennsylvanian limestones in the Orogrande Basin, New Mexico: water/rock interactions and basin geothermics: Journal of Sedimentary Petrology, v. 62, p. 652–670.

Allan, J. R., and Matthews, R. K., 1982, Isotopic signatures associated with early meteoric diagenesis: Sedimentology, v. 29, p. 797–817.

Beier, J. A., 1987, Petrographic and geochemical analysis of caliche profiles in a Bahamian Pleistocene dune: Sedimentology, v. 34, p. 991–998.

Berger, A., 1988, Milankovitch theory and climate: Reviews of Geophysics, v. 26, p. 624–657.

Berner, R. A., 1991, A model for atmospheric CO_2 over Phanerozoic time: American Journal of Science, v. 291, p. 339–376.

Berner, R. A., 1994, Geocarb II: a revised model of atmospheric CO_2 over Phanerozoic time: American Journal of Science, v. 294, p. 56–91.

Boardman, D. R., II, and Heckel, P. H., 1989, Glacial-eustatic sea-level curve for early Late Pennsylvanian sequence in north-central Texas and biostratigraphic correlation with curve for mid-continent North America: Geology, v. 17, p. 802–805.

Brown, A., 1982, Intraformational subaerial exposure of carbonates in the Canyon Group (Pennsylvanian), north-central Texas—evidence for eustatic control of facies distribution on the eastern shelf of the Midland Basin, *in* Cromwell, D. W., ed., Middle and Upper Pennsylvanian System of north-central and west Texas: Permian Basin Section, Society of Economic Paleontologists and Mineralogists, Publication 82-21, p. 201–214.

Budd, D. A., and Land, L. S., 1990, Geochemical imprint of meteoric diagenesis in Holocene ooid sand, Schooner Cays, Bahamas—correlation of calcite cement geochemistry with extant groundwaters: Journal of Sedimentary Petrology, v. 60, p. 361–378.

Caputo, M. V., and Crowell, J. C., 1985, Migration of glacial centers across Gondwana during Paleozoic Era: Geological Society of America Bulletin, v. 96, p. 1020–1036.

Cerling, T. E., 1991, Carbon dioxide in the atmosphere: evidence from Cenozoic and Mesozoic paleosols: American Journal of Science, v. 291, p. 377–400.

Cerling, T. E., Wang, Y., and Quade, J., 1993, Expansion of C4 ecosystems as an indicator of global ecological change in the late Miocene: Nature, v. 361, p. 344–345.

Connolly, W. M., and Stanton, R. J., Jr., 1992, Interbasinal cyclostratigraphic correlation of Milankovitch band transgressive-regressive cycles: correlation of Desmoinesian-Missourian strata between southeastern Arizona and the midcontinent of North America: Geology, v. 20, p. 999–1002.

Crowley, T. J., and Baum, S. K., 1991, Estimating Carboniferous sea-level fluctuations from Gondwanan ice extent: Geology, v. 19, p. 975–977.

Degens, E. T., 1969, Biogeochemistry of stable carbon isotopes, *in* Eglinton, G., and Murphy, M. T. J., eds., Organic geochemistry: New York, Springer, p. 304–329.

Deines, P., 1980, The isotopic composition of reduced organic carbon, *in* Fritz, P., and Fontes, J. C., eds., Handbook of environmental isotope geochemistry, Volume 1: Amsterdam, Elsevier, p. 329–406.

Denham, C. R., and Scotese, C. R., 1988, Terra Mobilis—A plate tectonics program for the Macintosh: Houston, Texas, Earth in Motion Technology, version 2.1.

Driese, S. G., Mora, C. I., and Walker, K. R., eds., 1992, Paleosols, paleoweathering surfaces, and sequence boundaries: University of Tennessee Department of Geological Sciences Studies in Geology 21, 111 p.

Frakes, L. A., 1979, Climates throughout geologic time: Amsterdam, Elsevier, 310 p.

Goetz, L. K., and Dickerson, P. W., 1985, A Paleozoic transform margin in Arizona, New Mexico, West Texas and Mexico, *in* Dickerson, P. W., and Muehlberger, W. R., eds., Structure and Tectonics of Trans-Pecos Texas: Midland, Texas, West Texas Geological Society, p. 173–184.

Goldhammer, R. K., Oswald, E. J., and Dunn, P. A., 1991, Heirarchy of stratigraphic forcing: example from Middle Pennsylvanian shelf carbonates of the Paradox basin, *in* Franseen, E. K., et al., eds., Sedimentary modeling: Computer simulations and methods for improved parameter definition: Kansas Geological Survey Bulletin 233, p. 361–413.

Goldstein, R. H., 1991, Stable isotope signatures associated with palaeosols, Pennsylvanian Holder Formation, New Mexico: Sedimentology, v. 38, p. 67–77.

Harland, W. B., Armstrong, R. L., Cox, A. V., Craig, L. E., Smith, A. G., and Smith, D. G., 1990, A geologic time scale 1989: Cambridge, Cambridge University Press, 263 p.

Heckel, P. H., 1986, Sea-level curve for Pennsylvanian eustatic marine transgressive-regressive depositional cycles along midcontinent outcrop belt, North America: Geology, v. 14, p. 330–334.

Klein, G. deV., 1990, Pennsylvanian time scales and cycle periods: Geology, v. 18, p. 455–457.

Kottlowski, F. E., 1963, Paleozoic and Mesozoic strata of southwestern and south-central New Mexico: New Mexico Bureau of Mines and Mineral Resources Bulletin 79, 100 p.

Langenheim, R. L., Jr., 1991, Pennsylvanian time scales and cycle periods: Comment: Geology, v. 19, p. 405–406.

Lohmann, K. C, 1988, Geochemical patterns of meteoric diagenetic systems and their application to studies of paleokarst, *in* James, N. P., and Choquette, P. W., eds., Paleokarst: New York, Springer, p. 58–80.

Lowenstam, H. A., 1961, Mineralogy, $^{18}O/^{16}O$ ratios, and strontium and magnesium contents of Recent and fossil brachiopods and their bearing on the history of the oceans: Journal of Geology, v. 69, p. 241-260.

Matthess, G., 1982, The properties of groundwater: New York, Wiley, 406 p.

Meyers, W. J., and Lohmann, K. C, 1985, Isotope geochemistry of regionally extensive calcite cement zones and marine components in Mississippian limestones, New Mexico, *in* Schneidermann, N., and Harris, P. M., eds., Carbonate cements: Society of Economic Paleontologists and Mineralogists Special Publication 36, p. 223–239.

Morgan, M. E., Kingston, J. D., and Marino, B. D., 1994, Carbon isotopic evidence for the emergence of C4 plants in the Neogene from Pakistan and Kenya: Nature, v. 367, p. 162–165.

Osleger, D., and Read, J. F., 1991, Relation of eustasy to stacking patterns of meter-scale carbonate cycles, Late Cambrian, U.S.A.: Journal of Sedimentary Petrology, v. 61, p. 1225–1252.

Pisias, N. G., and Shackleton, N. J., 1984, Modelling the global climate response to orbital forçing and atmospheric carbon dioxide changes: Nature, v. 310, p. 757–759.

Popp, B. N., Anderson, T. F., and Sandberg, P. A., 1986, Brachiopods as indicators of original isotopic compositions in some Paleozoic limestones: Geological Society of America Bulletin, v. 97, p. 1262–1269.

Popp, B. N., Takigiku, R., Hayes, J. M., Louda, J. W., and Baker, E. W., 1989, The post-Paleozoic chronology and mechanism of ^{13}C depletion in primary marine organic matter: American Journal of Science, v. 289, p. 436–454.

Posamentier, H. W., Jervey, M. T., and Vail, P. R., 1988, Eustatic controls on clastic deposition I—conceptual framework, *in* Wilgus, C. K., et al., eds., Sea-level changes: An integrated approach: Society of Economic Paleontologists and Mineralogists Special Publication 42, p. 109–124.

Pray, L. C., 1961, Geology of the Sacramento Mountains escarpment, Otero County, New Mexico: New Mexico Bureau of Mines and Mineral Resources Bulletin 35, 144 p.

Ramsbottom, W. H. C., 1979, Rates of transgression and regression in the Carboniferous of NW Europe: Geological Society of London Journal, v. 136, p. 147–153.

Read, J. F., Osleger, D., and Elrick, M., 1991, Two-dimensional modeling of carbonate ramp sequences and component cycles, *in* Franseen, E. K., et al., eds., Sedimentary modeling: Computer simulations and methods for improved parameter definition: Kansas Geological Survey Bulletin 233, p. 473–488.

Romanek, C. S., Grossman, E. L., and Morse, J. W., 1992, Carbon isotopic fractionation in synthetic aragonite and calcite: effects of temperature and precipitation rate: Geochimica et Cosmochimica Acta, v. 56, p. 419–430.

Ross, C. A., and Ross, J. R. P., 1985a, Paleozoic tectonics and sedimentation in West Texas, southern New Mexico and southern Arizona, *in* Dickerson, P. W., and Muehlberger, W. R., eds., Structure and tectonics of Trans-Pecos Texas: Midland, Texas, West Texas Geological Society, p. 221–230.

Ross, C. A., and Ross, J. R. P., 1985b, Late Paleozoic depositional sequences are synchronous and worldwide: Geology, v. 13, p. 194–197.

Saller, A. H., and Moore, C. H., Jr., 1991, Geochemistry of meteoric calcite cements in some Pleistocene limestones: Sedimentology, v. 38, p. 601–621.

Sarg, J. F., 1988, Carbonate sequence stratigraphy, *in* Wilgus, C. K., et al., eds., Sea-level changes: An integrated approach: Society of Economic Paleontologists and Mineralogists Special Publication 42, p. 155–181.

Snedecor, G. W., and Cochran, W. G., 1967, Statistical methods (sixth edition): Ames, Iowa, Iowa State University Press, 593 p.

Vail, P. R., 1987, Seismic stratigraphy interpretation using sequence stratigraphy, Part 1: Seismic stratigraphy interpretation procedure, *in* Bally, A. W., ed., Atlas of seismic stratigraphy: American Association of Petroleum Geologists Studies in Geology 27, p. 1–10.

Van Wagoner, J. C., Posamentier, H. W., Mitchum, R. M., Vail, P. R., Sarg, J. F., Loutit, T. S., and Hardenbol, J., 1988, An overview of sequence stratigraphy and key definitions, *in* Wilgus, C. K., et al., eds., Sea-level changes: An integrated approach: Society of Economic Paleontologists and Mineralogists Special Publication 42, p. 39–45.

Van Wagoner, J. C., Mitchum, R. M., Campion, K. M., and Rahmanian, V. D., 1990, Siliciclastic sequence stratigraphy in well logs, cores, and outcrops: American Association of Petroleum Geologists Methods in Exploration Series 7, 55 p.

Veevers, J. J., and Powell, C. M., 1987, Late Paleozoic glacial episodes in Gondwanaland reflected in transgressive-regressive depositional sequences in Euramerica: Geological Society of America Bulletin, v. 98, p. 475–487.

Veizer, J., Fritz, P., and Jones, B., 1986, Geochemistry of brachiopods—oxygen and carbon isotopic records of Paleozoic oceans: Geochimica et Cosmochimica Acta, v. 50, p. 1679–1696.

Wilson, J. L., 1975, Carbonate facies in geologic history: New York, Springer, 471 p.

MANUSCRIPT ACCEPTED BY THE SOCIETY SEPTEMBER 12, 1995